GEOLOGICAL SURVEY OF CANADA
OPEN FILE 7853

Targeted Geoscience Initiative 4: Contributions to the Understanding of Volcanogenic Massive Sulphide Deposit Genesis and Exploration Methods Development

Volcanic architecture and alteration assemblages of the Ming Cu-Au-(Zn-Ag) VMS deposit, Baie Verte, Newfoundland and Labrador: Implications for Au-enrichment processes and exploration

Jean-Luc Pilote[1], Stephen J. Piercey[1], and Patrick Mercier-Langevin[2]

[1]Memorial University of Newfoundland, St. John's, Newfoundland and Labrador
[2]Geological Survey of Canada, Québec, Quebec

2015

Recommended citation

Pilote, J.-L., Piercey, S.J., and Mercier-Langevin, P., 2015. Volcanic architecture and alteration assemblages of the Ming Cu-Au-(Zn-Ag) VMS deposit, Baie Verte, Newfoundland and Labrador: Implications for Au-enrichment processes and exploration, *In:* Targeted Geoscience Initiative 4: Contributions to the Understanding of Volcanogenic Massive Sulphide Deposit Genesis and Exploration Methods Development, (ed.) J.M. Peter and P. Mercier-Langevin; Geological Survey of Canada, Open File 7853, p. 197–210.

Publications in this series have not been edited; they are released as submitted by the author.

Contribution to the Geological Survey of Canada's Targeted Geoscience Initiative 4 (TGI-4) Program (2010–2015)

TABLE OF CONTENTS

Volcanic architecture and alteration assemblages of the Ming Cu-Au-(Zn-Ag) VMS deposit, Baie Verte, Newfoundland and Labrador: Implications for Au-enrichment processes and exploration

Jean-Luc Pilote[1], Stephen J. Piercey[1]*, and Patrick Mercier-Langevin[2]

[1]Department of Earth Sciences, Memorial University of Newfoundland, St. John's, Newfoundland and Labrador A1B 3X5
[2]Geological Survey of Canada, 490 rue de la Couronne, Québec, Quebec G1K 9A9
*Corresponding author's e-mail: spiercey@mun.ca

ABSTRACT

The Ming deposit is hosted in Cambro-Ordovician intermediate to felsic rocks underlain by ca. 490 Ma ophiolite slivers of boninitic composition. The deposit consists of five elongated semi-massive to massive sulphide lenses that plunge 30º to the northeast and occur in the uppermost part of a calc-alkalic intermediate to felsic volcanic succession. The immediate hanging wall varies from mafic volcanic breccia to magnetite-rich volcanogenic siltstone. Three generations of mafic to intermediate intrusive rocks are present in the deposit; they each have distinctive lithogeochemical signatures and are interpreted to be genetically related to the mafic rocks of the cover sequence.

The Ming deposit has seven distinct alteration mineral assemblages (from proximal to distal from mineralization): quartz-pyrite, quartz-calcite-garnet, sericite-green mica-sulphide, sericite-quartz-pyrite, chlorite-amphibole-quartz, chlorite-sericite-quartz-sulphide, and chlorite-stringer zone assemblages. A chalcopyrite-pyrrhotite-pyrite stringer zone associated with the chlorite-stringer zone assemblage occurs 50–100 m stratigraphically below the Ming North and Ming South lenses, at what was the site of high-temperature fluid discharge from a hydrothermal system. The spatial and temporal geological relationships between the stratigraphic package, alteration styles, mineralization, and deformation strongly support a syngenetic origin for mineralization and Au-enrichment.

INTRODUCTION

The Ming deposit is a Au-Ag-bearing volcanogenic massive sulphide (VMS) deposit located in the Baie Verte Peninsula in northern Newfoundland, which is part of the Notre-Dame subzone of the Canadian Appalachian orogen (Fig. 1). The deposit is part of a group of four past and currently producing precious metal-rich VMS deposits that collectively are known as the consolidated Rambler and Ming mining camp (herein referred to as the Rambler camp). The Rambler camp deposits are hosted by the ca. 489–487 Ma upper Pacquet Complex, part of the Baie Verte Oceanic Tract (Fig. 2; van Staal and Barr, 2012; van Staal et al., 2013). The Ming deposit consists of five Cu-Au-Zn-Ag-rich, semi-massive to massive pyrite-rich lenses, veins, and stringer zones located within variously sericite-chlorite-quartz-altered intermediate to felsic volcanic rocks with a large proportion of volcaniclastic rocks. These zones are, from the northwest to the southeast, the 1807, 1806, Ming North, Ming South, and Lower Footwall zones (Fig. 3). The current combined past production, reserves, and measured, indicated, and inferred resources at Ming are estimated at 35.44 Mt grading 1.56 wt% Cu, 0.1 wt% Zn, 2.6 g/t Ag, and 0.42 g/t Au (Rambler Metals and Mining, press releases, January 27, 2014 and November 27, 2014). The base and precious metal contents vary among these zones (Fig. 4) with the highest Au grades in the 1806 zone (measured resources of 267,000 tonnes at 0.56 wt% Cu, 1.31 wt% Zn, 32.15 g/t Ag, and 4.31 g/t Au), which puts it into the subclass of "auriferous" VMS deposits (Poulsen and Hannington, 1995; Poulsen et al., 2000; Mercier-Langevin et al., 2011; Brueckner et al., 2014a).

The timing and mode of Au-Ag introduction in ancient VMS deposits in general, including Ming, is debated due to modifications to the primary features through superimposed deformation and metamorphism (e.g. Mercier-Langevin et al., 2015); this lack of agreement has hampered the improvement of exploration models. In this study, we describe the geology of the Ming deposit and recently discovered precious metal-rich zones, the hydrothermal alteration, and the geochemical composition of the host rocks in order to con-

Pilote, J.-L., Piercey, S.J., and Mercier-Langevin, P., 2015. Volcanic architecture and alteration assemblages of the Ming Cu-Au-(Zn-Ag) VMS deposit, Baie Verte, Newfoundland and Labrador: Implications for Au-enrichment processes and exploration, *In:* Targeted Geoscience Initiative 4: Contributions to the Understanding of Volcanogenic Massive Deposit Sulphide Genesis and Exploration Methods Development, (ed.) J.M. Peter and P. Mercier-Langevin; Geological Survey of Canada, Open File 7853, p. 197–210.

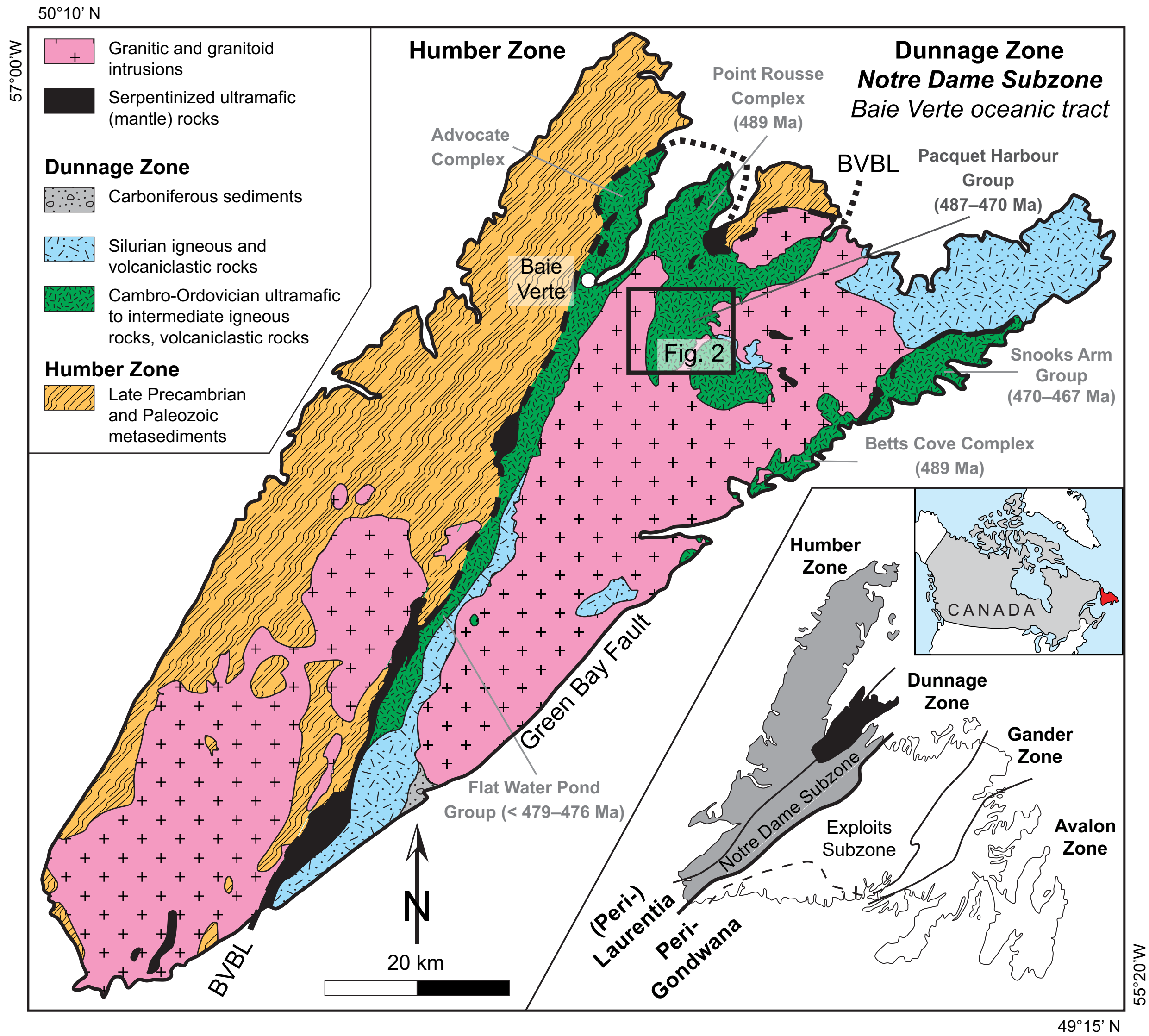

Figure 1. Simplified geological map of the Baie Verte Peninsula (modified from Skulski et al., 2010) showing the (peri-) Laurentian (inset: in grey) and (peri-)Gondwanan tectonostratigraphic zones that form the Appalachian orogenic belt in Newfoundland (Williams, 1979). Abbreviation: BVBL = Baie Verte-Brompton Line.

strain the timing and processes of precious metal-enrichment to develop improved genetic and exploration models.

REGIONAL GEOLOGY

The Ming deposit is hosted by intermediate to felsic rocks of the informally named Rambler Rhyolite formation (Skulski et al., 2010), which consists of a 6 km-wide and 2.5 km-thick folded dome-shaped sequence of quartz-phyric rhyodacite, felsic tuff and tuff breccia, striking northwest and dipping 30º (Fig. 3; Hibbard, 1983; Castonguay et al., 2009). Rhyolite immediately stratigraphically below the nearby Rambler Main deposit yielded a U-Pb zircon age of 487 ± 4 Ma (Fig. 2; Skulski et al., 2010). Stratigraphically below the Rambler Rhyolite formation is low-Ti boninite intercalated with thin (<50 m) beds of felsic tuff and rhyodacite flows (Hibbard, 1983; Piercey et al., 1997; Skulski et al., 2010) of the Betts Head Formation (Skulski et al., 2010), which hosts the Big Rambler Pond (Fig. 2) and the Tilt Cove and Betts Cove VMS deposits (Fig. 1). Stratigraphically overlying the Betts Head Formation are intermediate Ti boninite, island arc tholeiitic pillow basalt, breccia, and minor felsic tuff, which are part of the Mount Misery Formation (Skulski et al., 2010). The upper part of this sequence is structurally repeated in the hanging wall of the Rambler Brook Fault (Fig. 2; Castonguay et al., 2009) where it hosts the Rambler Rhyolite formation and the massive sulphide lenses of the Ming deposit. The Rambler Rhyolite formation is locally overlain by thin lenses of basalt of island-arc affinity that are chemically similar to those of the Mount Misery Formation (Skulski et al., 2010). The latter are overlain by the ca. 479–467 Ma

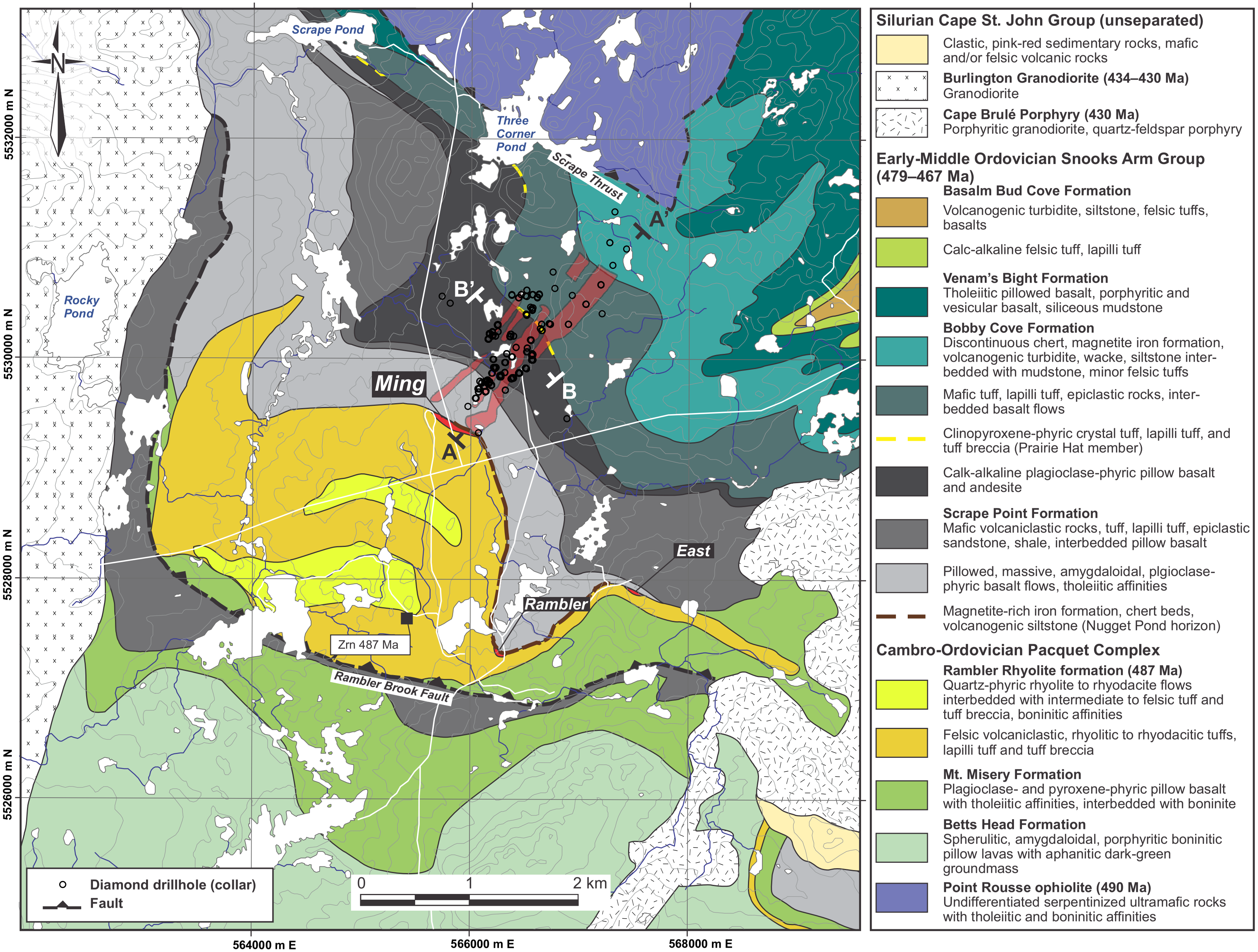

Figure 2. Geological map of the study area, Baie Verte Peninsula, with Ming VMS orebodies projected to surface and shown in light red. Datum is UTM 21N NAD 83. Map compiled and modified from Tuach and Kennedy (1978), Hibbard (1983), Castonguay et al. (2009), Pilgrim (2009), and Skulski et al. (2010). Ages are from Cawood et al. (1993), Castonguay et al. (2009), and Skulski et al. (2010).

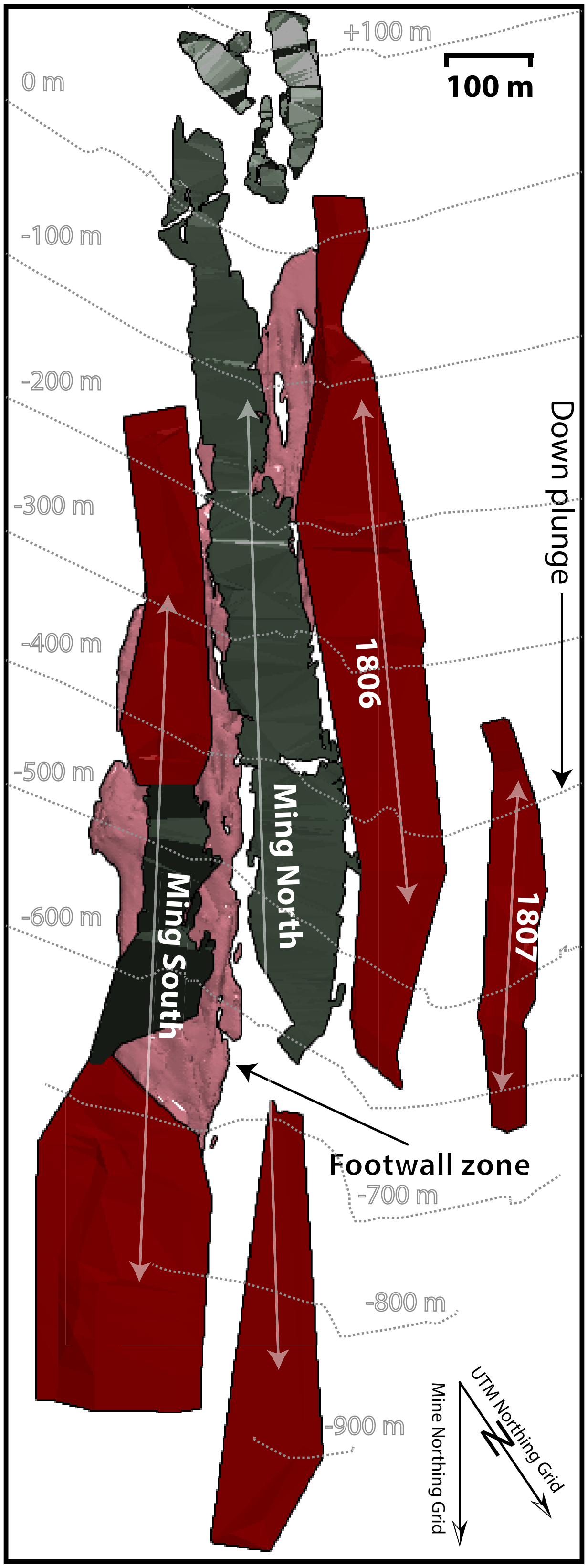

Figure 3. Plan view of a 3-D model of the Ming orebodies projected to surface (0 m). The surface of wireframes in red represent orebodies currently in production or those that will be mined, whereas those in grey were mined in the past. Mine north is 34° east of UTM north. Model modified from Pilgrim (2009).

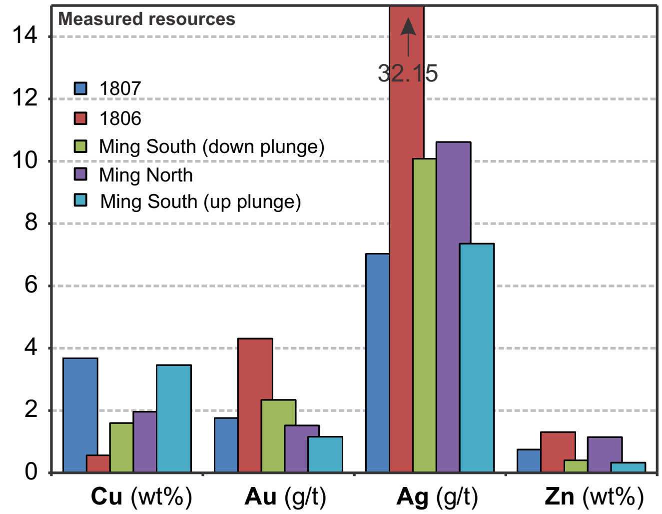

Figure 4. Measured resources of Cu (wt%), Au (g/t), Ag (g/t), and Zn (wt%) for the 1807, 1806, Ming South (down and up plunge), and Ming North zones. Data from Pilgrim (2009).

Snooks Arm Group, which is the cover sequence to the Pacquet Complex. The base of the Snooks Arm Group consists of a thin (<1 m) sequence of chert, magnetite-rich mudstone to siltstone, and sandstone (Nugget Pond horizon). This sequence is laterally extensive and is present throughout the Baie Verte Peninsula (Skulski et al., 2010). Overlying this unit are thin (<1 m) to thick (>100 m) alternating sequences of volcaniclastic monomictic to polymictic conglomerate, epiclastic wacke, iron formation, high-Ti tholeiitic to calc-alkaline basalt, and mafic to felsic volcaniclastic rocks (Hibbard, 1983; Skulski et al., 2010).

DEPOSIT GEOLOGY

The stratigraphic footwall of the deposit is composed of three main volcanic and volcaniclastic units (classified following the nomenclature of White and Houghton, 2006).

The lower part of the stratigraphic footwall at Ming (Fig. 5) is dominated by quartz-phyric rhyodacite (Fig. 6a), with minor intercalated beds of fine rhyodacitic tuff to coarse lapilli tuff (unit 1.1). This unit has a minimum thickness of 150 m and has gradational to sharp contacts with the flows. The rhyodacite is massive with up to 15 vol.% quartz phenocrysts (≤5 mm in size). Overlying unit 1.1 is a sequence predominantly composed of volcaniclastic rocks (unit 1.2) that range from a dominantly fine tuff in the southeast (Ming South zone) to a tuff breccia in the northwest (1807 zone) (Fig. 6b, c). Unit 1.2 is ~100 m thick and consists of several volcaniclastic sequences with subrounded and intermediate tuffaceous fragments that are elongated due to deformation. Quartz porphyroclasts occur both in the matrix and the latter fragments with similar abundance to rocks of unit 1.1. Units 1.1 and 1.2 contain discordant sulphide stringer veins, such as the

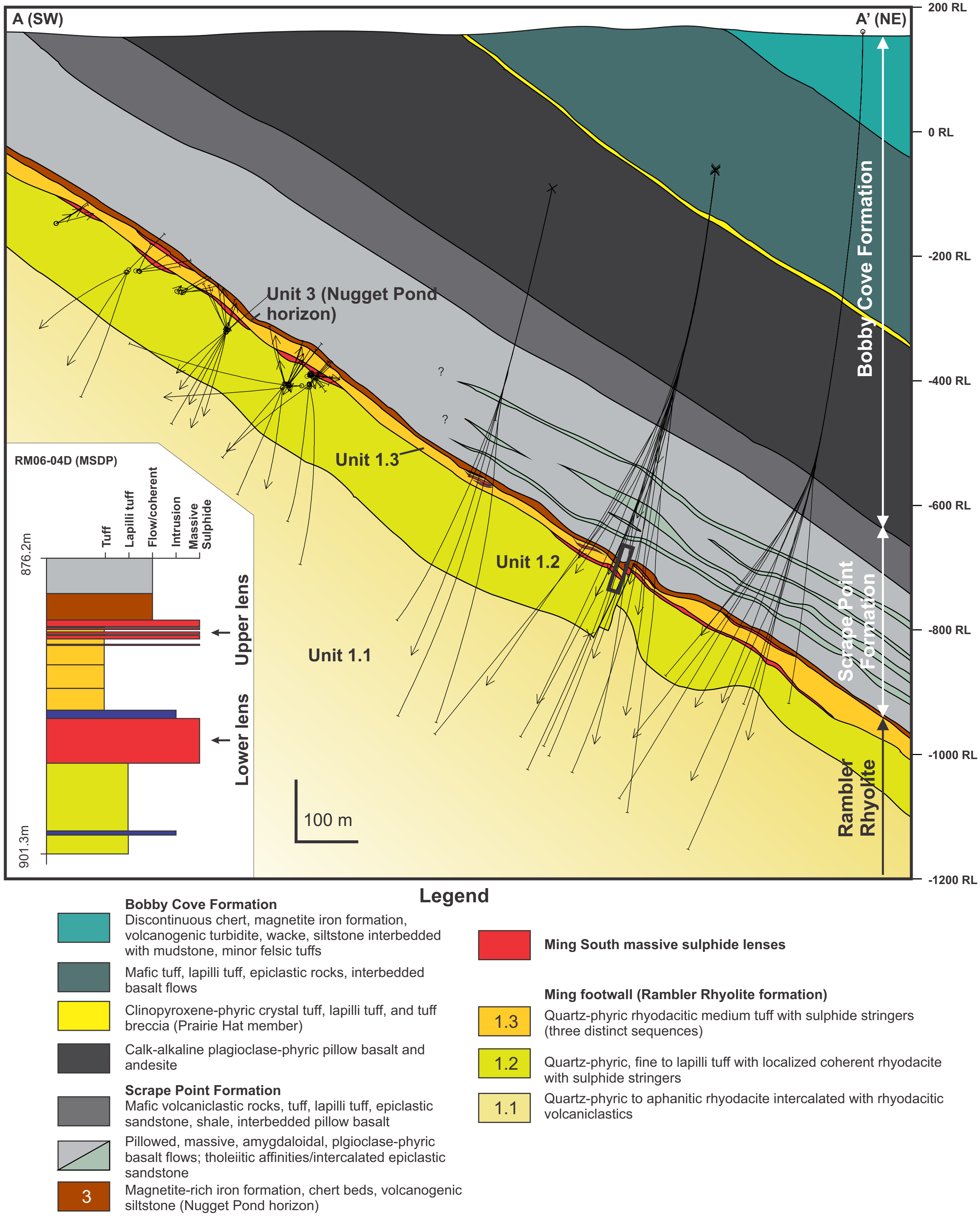

Figure 5. Simplified geological cross-section of the Ming South zone (looking southwest). The black lines represent drillhole traces from which the geology was interpreted. The dykes were omitted to simplify the map. Units 1.1, 1.2, 1.3, and 2 are described in the text. The inset shows the stratigraphy close to the mineralization from a representative drillhole (location indicated by the black box). Unit names are from Skulski et al. (2010). The Ming North, 1806, and 1807 lenses have not been depicted as they occur northwest of this cross-section.

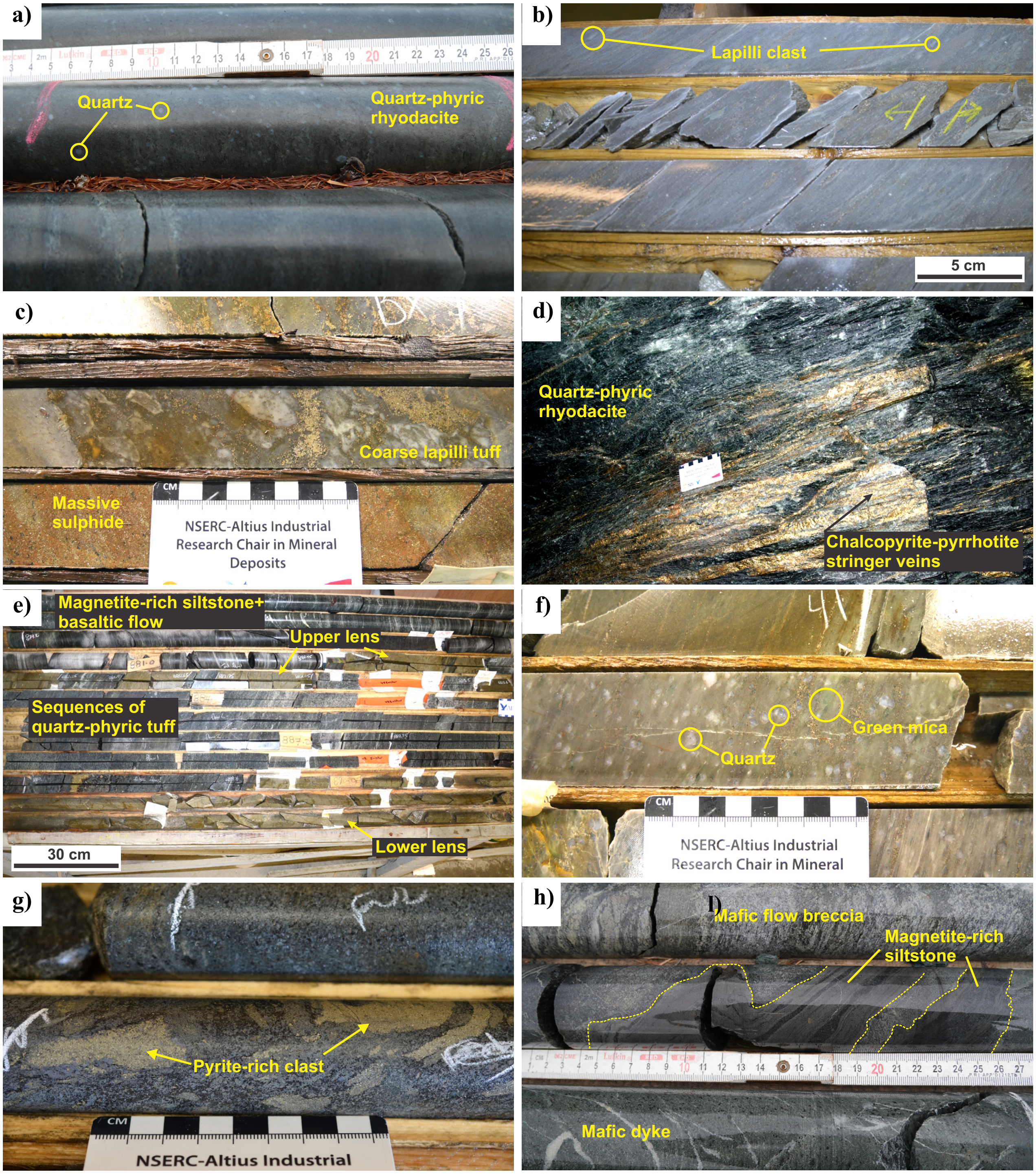

Figure 6. Representative and selected underground and drillcore photographs of the rock units that comprise the Ming footwall. **a)** Coherent quartz-phyric rhyodacite from the Ming North footwall (unit 1.1; DDH RM09-22, 612.5 m depth). Scale is in cm. **b)** Rhyodacitic tuff to lapilli tuff typical of the Ming South zone footwall (unit 1.2; DDH RM04-04, 1036.5 m depth). **c)** Coarse lapilli tuff with the matrix replaced by sulphides from immediately below the 1806 massive sulphide lens (unit 1.2; DDH RMUG08-140; 40.5 m depth). Scale is in cm. **d)** Transposed sulphide (chalcopyrite+pyrrhotite) stringer veins cutting a quartz-phyric rhyodacite in the Lower Footwall zone (1450 level). Scale is in cm. **e)** Drillcore intersection showing the upper and lower sulphide lenses of the Ming South zone, separated by quartz-phyric tuff beds. The upper lens is overlain by magnetite-rich siltstone and basalt (unit 1.3; DDH RM06-04D, starting at 876.2 m depth). **f)** Quartz-bearing rhyodacitic tuff with minor green mica, which is representative of unit 1.3, between the lower and upper sulphide lenses of the Ming South zone (DDH RMUG08-25, 42.5 m depth). **g)** Polymictic mafic tuff breccia with up to 20 vol.% pyrite-rich clasts. This unit occurs above the 1806 and 1807 zones (unit 2; DDH RMUG13-205, 34 m depth). Scale is in cm. **h)** Folded magnetite-rich siltstone bed part of the Nugget Pond horizon (unit 3), overlain by a mafic flow breccia. This unit is extensive and occurs at or near the contact with the Ming deposit (DDH RM09-22, 40 m depth). Scale is in cm. Abbreviation: DDH = diamond drillhole

Table 1. Characteristics of the alteration assemblages in the Ming deposit.

Mineralogical assemblage	Main minerals (vol %)	Associated minerals (minor and traces)	Distribution
1. Quartz-pyrite	Quartz (≤90%), pyrite (≤10%)	Green mica	Immediately above and below the massive sulphide of the 1806 and 1807 zones
2. Quartz-calcite-garnet	Quartz (≤40%), Calcite (≤20%), garnet (≤40%)	Epidote (≤10%)	1807 zone to a maximum depth of 10 m
3. Sericite-green mica-pyrite	Sericite (≤40%), green mica (≤30%), pyrite (≤20%), quartz (≤10%)	Biotite, garnet, magnetite, chalcopyrite, sphalerite, galena, electrum, sulfosalts, tellurides	In all zones to a depth of 30 m
4. Sericite-quartz-pyrite	Sericite (≤45%), quartz (≤40%), pyrite (≤5%)	Sphalerite, biotite, epidote, ilmenite, rutile, and chlorite	1806, Ming North, Ming South to a maximum depth of 50 m
5. Chlorite-actinolite-quartz	Chlorite (≤40%), actinolite (≤20%), quartz (≤20%)	Epidote (≤10%), biotite (≤10%)	Sporadically throughout all zones but mainly 1806, Ming North and Ming South
6. Chlorite-sericite-quartz-sulphide	Chlorite (≤45%), sericite (≤45%), quartz (≤10%)	Biotite, epidote, apatite, pyrite, chalcopyrite, pyrrhotite	Below Ming South and Ming North at a minimum depth of 50 m
7. Chlorite-stringer zone	Chlorite (≤45%), quartz (≤45%)	Biotite, epidote, actinolite, titanite, apatite, zircon, epidote, chalcopyrite, pyrrhotite, pyrite, Bi-telluride	Below Ming South and Ming North at a minimum depth of 50 m

Lower Footwall zone (Fig. 6d), and stratiform to discordant semi-massive to massive sulphides. The semi-massive to massive sulphide lenses have a maximum thickness of 11 m (average ~4 m) consisting of >30 metal-bearing minerals (Brueckner et al., 2014b) and quartz gangue, with the most common sulphides being pyrite, chalcopyrite, pyrrhotite, and sphalerite.

The Ming South zone contains two stratabound and stratiform massive sulphide lenses separated by three ≤10 m-thick discrete beds of rhyodacitic tuff (unit 1.3; Fig. 6e). The tuff beds are quartz-bearing (Fig. 6f), light to dark grey, and are cut by chalcopyrite-pyrite-quartz stringer veins (<2 vol. % of the rock). The upper and lower sulphide lenses in the Ming South zone have different mineral assemblages; the lower lens has chalcopyrite, sphalerite, and galena, whereas the upper lens has pyrite and chalcopyrite. The grades in the lower lens average 3.58 wt% Cu and 4.8 g/t Au, and the upper lens averages 0.78 wt% Cu and 1.2 g/t Au (averaged sulphide assays from five diamond drillholes; RM06-04c, d, e, g, and RM05-09, L. Pilgrim, unpublished data, 2015), in agreement with the dominant sulphide mineralogy.

The massive sulphides in the 1806 and 1807 zones are immediately stratigraphically overlain by a dark grey mafic tuff breccia with sulphide clasts (unit 2; Fig. 6g). The matrix is fine-grained and biotite-rich that contains fragments of medium-grained pyrite-quartz clasts, quartz-altered aphanitic felsic volcanic clasts, and epidote-altered mafic volcanic clasts. The fragments are subrounded, elongated, and up to 5 cm in length. Unit 2 is overlain by the regionally extensive magnetite-rich siltstone (unit 3; Fig. 6h).

Three generations of mafic to intermediate sills and dykes have intruded the deposit, and they crosscut all styles of mineralization. Each dyke generation has a distinctive lithogeochemical signature (Pilote et al., 2014). The dykes have similar geochemical affinities as the rocks of the Snooks Arm Group (J.-L. Pilote, unpublished data, 2014) and are cogenetic with them.

The Baie Verte Peninsula was affected by three phases of regional deformation, but only the last two are recognized at Ming. In the deposit, the D_2 deformation is defined by an east-west-striking cleavage to a penetrative schistosity (S_2) that is axial-planar to megascopic east-trending open to tight F_2 folds, with strong L > S fabrics. The north-dipping, south-directed Rambler Brook Fault and Scrape Thrust (Fig. 2) are interpreted to be D_2 structures (Castonguay et al., 2009). The D_3 deformation is characterized by open, upright cross folds with axial planes trending north-northeast. The elongated morphology of the orebodies (Fig. 2 and 3) is in large part due to the S_2 stretching (L_2) and superimposed effect of D_3 deformation (Castonguay et al., 2009).

HYDROTHERMAL ALTERATION ASSEMBLAGES

The Ming stratigraphic footwall rocks contain seven alteration assemblages that have distinctive mineralogies and relative abundances of key minerals (Table 1), with a strong lateral and vertical alteration zonation. Immediately above and below the 1806 and 1807 zone massive sulphide lenses, the rocks have grey quartz-pyrite alteration (Fig. 7a), with samples containing up to 92 wt% SiO_2 (J.-L. Pilote, unpublished data, 2014).

The footwall of the 1807 zone contains a distinct salmon-pink quartz-calcite-Mn-rich garnet alteration assemblage that extends up to 10 m stratigraphically below the massive sulphides (Fig. 7b and 8). This mineral assemblage comprises fine-grained (≤100 μm) polygonal quartz and idioblastic garnet. This alteration overprints a sericite-quartz-altered, quartz-bearing, medium-grained felsic tuff (unit 1.2).

A sericite-green mica-sulphide assemblage occurs in all zones within 30 m of the massive sulphide lenses (Fig. 7c). This alteration assemblage is cut by discordant stringers of pyrite-chalcopyrite-sphalerite-galena with trace electrum, sulphosalts, and tellurides (up to 10 vol.%). This assemblage also contains trace euhedral magnetite and syn-D_2 garnet and biotite porphyroblasts. Green mica is more abundant in the Au-rich 1806 zone (≤30 vol.%) than in the other zones (≤5 vol.%). Preliminary lithogeochemical analyses indicate that green mica-bearing rocks have a higher Cr content (~1600 ppm) than the surrounding sericite-rich rock (~100 ppm) (J.-L. Pilote, unpublished data, 2014).

Sericite-quartz-pyrite alteration is present in the 1806, Ming North, and Ming South zones up to ~50 m stratigraphically below the massive sulphide lenses (Fig. 7d). The assemblage is dominated by sericite, quartz, and disseminated anhedral pyrite with minor sphalerite, biotite, epidote, ilmenite, rutile, and chlorite. Sphalerite, pyrite, and ilmenite form thin (≤1 mm) discontinuous bands within this assemblage, whereas epidote, rutile, and biotite form hypidiomorphic porphyroblasts.

A chlorite-amphibole-quartz assemblage occurs in places throughout the footwall in all zones within 50 m stratigraphically below the massive sulphides (Fig. 7e). This assemblage predominantly occurs in volcaniclastic rocks and is composed of chlorite, actinolite, and quartz with subordinate epidote and biotite. The biotite and actinolite grains are porphyroblastic and actinolite is paragenetically later than biotite.

Below the Ming North and Ming South zones, a chlorite-sericite-quartz-sulphide alteration assemblage occurs mostly in the volcaniclastic rocks and is proximal to the chlorite-stringer zone assemblage (see below). This assemblage also contains minor biotite, epidote, and apatite. This assemblage also includes ≤5 mm-wide bands of fine-grained sericite and quartz veins that cut the chlorite-quartz-sulphide assemblage (Fig. 7f, g), and these bands themselves are cut by discordant <1 cm-wide pyrite, chalcopyrite, and pyrrhotite stringer veins.

Lastly, a pervasive chlorite-stringer zone alteration assemblage occurs 50 to 100 m stratigraphically below the Ming South and Ming North zones. This assemblage hosts the Lower Footwall stringer zone and is composed predominantly of chalcopyrite, pyrrhotite, pyrite, Bi-tellurides, chlorite, quartz, minor biotite, epidote, actinolite, titanite, apatite, and zircon (Fig. 7h). The sulphide minerals and Bi-tellurides form centimetre-scale stringer veins that are discordant and transposed into S_2.

DISCUSSION

Deposit Architecture and Preliminary Genetic Model

The nature and style of the ore and alteration of VMS deposits are partly controlled by the volcanic architecture of the host succession (Gibson et al., 1999). The Ming deposit is hosted by massive rhyodacitic and intercalated volcaniclastic rocks that grade upward into predominantly rhyodacitic volcaniclastic rocks where semi-massive to massive sulphide lenses occur. The vertical transition from unit 1.1 to 1.2 may reflect the evolution from a subaqueous flow-dome complex to an eruptive volcaniclastic succession, common for shallow marine environments and the setting of numerous VMS deposits (e.g. Allen et al., 1996; Franklin et al., 2005; Gibson, 2005; Ross and Mercier-Langevin, 2014). The lack of sedimentary rocks and/or laminated tuff in the footwall rocks (units 1.1 and 1.2) may be due to rapid emplacement and formation of the flow-dome complex.

The mineralization in the 1807, 1806, Ming North and Ming South (lower lens) zones are immediately stratigraphically underlain by a distinctive rhyodacitic fine tuff to lapilli tuff unit, suggesting that all sulphide zones formed contemporaneously. In the southeastern part of the deposit, a younger succession of intermediate tuff beds and pyrite-rich massive sulphides (upper lens) were deposited above sulphide lenses (Ming South and possibly Ming North), whereas in the northwestern part of the deposit, a sulphide-rich volcanic breccia succession was formed, possibly coeval with the deposition of unit 1.3. The occurrence of a sulphide-rich volcanic breccia succession may indicate either that flow-breccia or talus-breccia deposits formed on top, or at the margin, of the flow-dome complex, or it reflects the presence of a depression controlled by synvolcanic faulting.

Mineralization at Ming is hosted predominantly in volcaniclastic rocks, close to a flow-dome complex. This volcanic architecture is likely due to permeability contrasts between the coherent and volcaniclastic rocks (Pilote et al., 2014). The spatial distribution of the alteration assemblages (Fig. 8) reflects these lithofacies changes. The lithofacies changes together with the

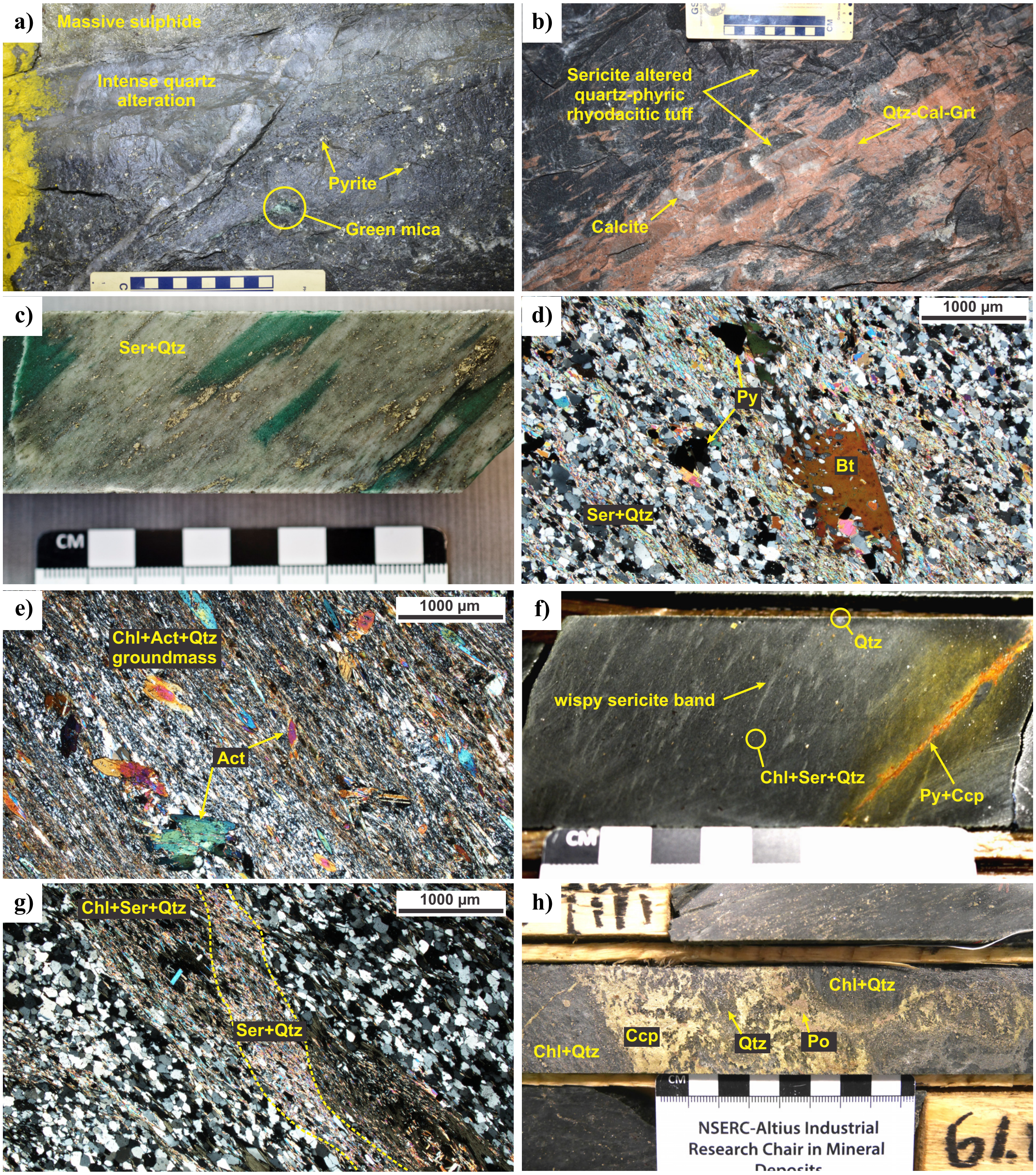

Figure 7. Representative and selected underground and drillcore photographs and photomicrographs of the different alteration styles that characterize the Ming footwall rocks. **a)** View looking south in level 329 (1807 zone) of the silica-pyrite alteration overprinting the weakly sericitized ±green mica rhyodacitic tuff. **b)** View looking southwest of a Mn-altered (Mn-garnet, quartz, and calcite) quartz-phyric rhyodacitic tuff underlying the massive sulphide (level 481, 1807 zone). **c)** Drillcore showing intense sericite-green mica-pyrite alteration in the 1806 zone (DDH RMUG14-261, 28.6 m depth). **d)** Photomicrograph illustrating the close relationship between quartz, sericite, disseminated pyrite, and biotite porphyroblasts in the sericite-quartz-pyrite alteration assemblage (sample 60553; DDH RM05-08, 1054 m depth). **e)** A fine-grained groundmass composed of chlorite-actinolite-quartz with randomly oriented actinolite porphyroblasts (sample 62515; DDH RM07-18, 729 m depth). **f)** Wispy sericite bands cutting an intense chlorite-sericite-quartz-altered quartz-phyric rhyodacite. These are in turn cut by a pyrite-chalcopyrite stringer vein (DDH RM05-08, 1275 m depth). **g)** A photomicrograph of (f) showing the relationship between the chlorite-sericite-quartz alteration assemblage cut by a later vein of sericite-quartz. **h)** Intense chlorite alteration cut by discordant chalcopyrite-pyrrhotite-quartz-rich veins, which is representative of the chlorite-stringer zone alteration assemblage (DDH RMUG14-250, 59.5 m depth). Abbreviations: Act = actinolite, Bt = biotite, Cal = calcite, Ccp = chalcopyrite, Chl = chlorite, Grt = garnet, Po = pyrrhotite, Py = pyrite, Qtz = quartz, Ser = sericite.

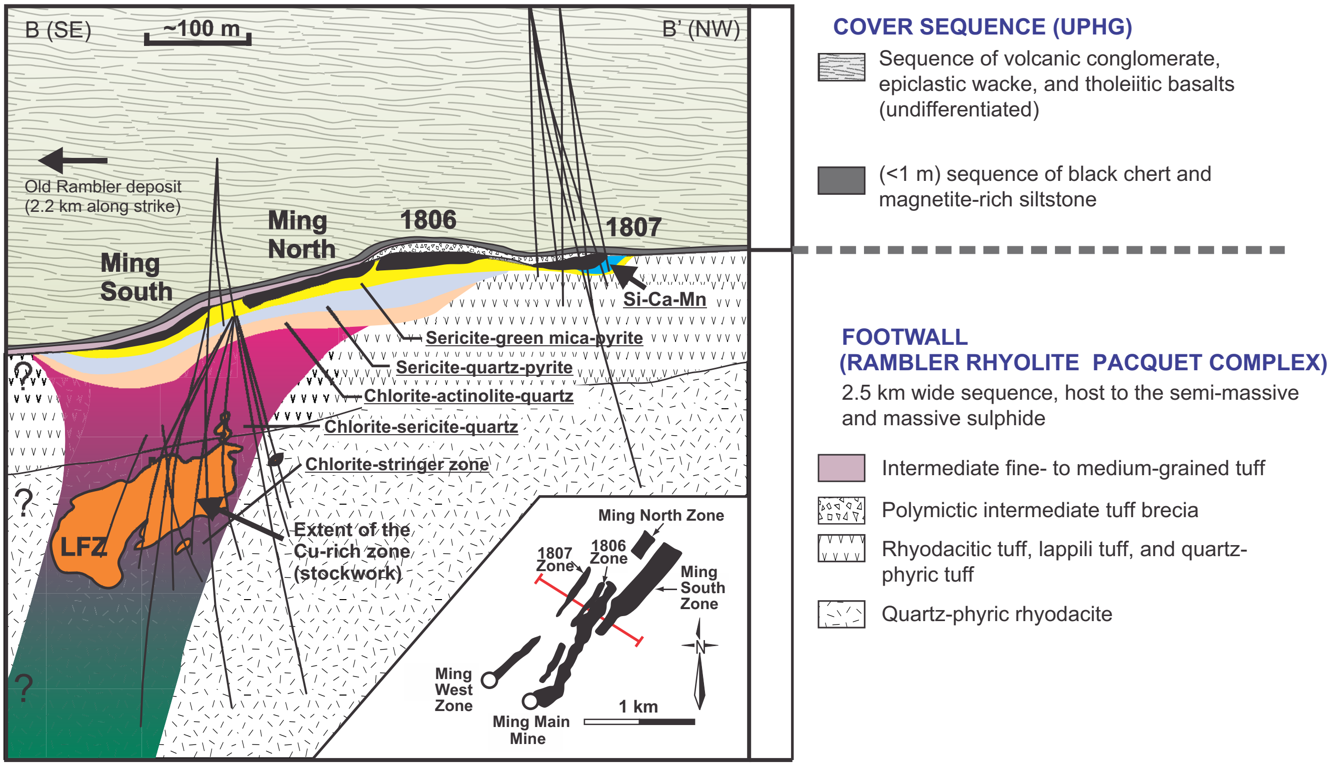

Figure 8. Simplified geological cross-section (looking southwest) of the Ming deposit. The distribution of the alteration assemblages (described in more detail in the text) was defined using petrographic, hyperspectral, and geochemical analyses (J.-L. Pilote, unpublished data, 2014) from numerous diamond drillholes (black lines) and underground mapping.

hydrothermal fluid conditions (i.e. temperature, pressure, pH, fO_2, and fS_2) were likely controlled by emplacement into relatively shallow water. The pervasive chlorite-stringer zone alteration assemblage that occurs adjacent to, and subparallel with, the Ming North and Ming South zones, and the discordant chalcopyrite-pyrite stringer veins indicate high-temperature fluid-rock interaction and ore deposition (>300ºC; e.g. Lydon, 1988; Ohmoto, 1996) in the Lower Footwall zone. No such alteration occurs stratigraphically below the 1806 and 1807 zones, indicating that these zones were formed from lower temperature fluids at potentially distal parts of the hydrothermal system (Fig. 8; Brueckner et al., 2014a). Within 50 m of massive sulphides, the alteration mineral assemblage is dominated by sericite and quartz, which is consistent with lower temperature alteration (Fig. 8; e.g. Lydon, 1988).

Timing of Mineralization and Gold Enrichment

Determining the timing of Au introduction into Au-enriched VMS (and modern seafloor massive sulphide) deposits is key to formulating and refining exploration models for such deposits and understanding their genesis. At Ming, multiple lines of evidence suggest Au-enrichment was synvolcanic: 1) the multiple strata-bound massive sulphide lenses occur at the same stratigraphic position (i.e. at the top of units 1.2 and 1.3), which reflects a stratigraphic control, thus favouring a syngenetic model of mineralization; 2) mafic to intermediate feeder dykes to the hanging-wall Snooks Arm Group crosscut the massive sulphides (Pilote and Piercey, 2013; Pilote et al., 2014). These dykes and rocks of the Snooks Arm Group postdate mineralization, are deformed, and are unmineralized, indicating that Au-enrichment was likely not due to a later structural and metamorphic overprint, as these post-mineralization rocks should display Au-enrichment as well if this were the case; 3) despite deposit-scale variations in Au and Ag contents, Au and Ag are almost exclusively confined to the massive sulphides, and only locally has Au remobilization into hosting volcanic rocks been documented (e.g. 1807 zone; Pilote et al., 2014). The massive sulphides and rocks above and below them are deformed with crosscutting structures that extend outside the deposit. These structures contain no Au, and this, together with the evidence presented in (2) above, suggests that the precious metals originated in the primary ore and were not introduced by a later orogenic overprint; and 4) the Au-enriched 1806 zone and parts of the 1807 and Ming South zones are enveloped by the synvolcanic sericite-green mica-sulphide alteration assemblage. Green mica is present in some VMS systems (e.g. Que River and Hellyer: Gemmell and Fulton, 2001; LaRonde-Penna: Dubé et al., 2007). Although the evidence is circumstantial, the close association between Au-enriched ore and green mica alteration in the 1806 zone at Ming may represent a key indicator to Au-rich mineralization. The relationship of this green mica alteration with the Au-enrichment process(es) at Ming is currently under investigation.

The Au-enrichment at Ming may originate from direct magmatic hydrothermal fluids containing Ag and Au. Based on the presence of abundant sulphosalts, including Ag-bearing tennantite-tetrahedrite, stannite, boulangerite, and loellingite, and precious metal-rich phases (tellurides, miargyrite, pyrargyrite, mercurian stephanite, unnamed AgCuFeS phase, Ag-Hg ± Au alloys), Brueckner et al. (2014a) concluded that the mineralization is of an intermediate-sulphidation type in which magmatic hydrothermal fluids containing volatiles and Au were introduced by magmatic degassing of a large rhyodacitic flow-dome complex in the immediate footwall to the deposit; this model is similar to that proposed at the LaRonde Penna deposit, Quebec (Mercier-Langevin et al., 2007).

IMPLICATIONS FOR EXPLORATION

Numerous geological field criteria from the Ming deposit can be used to determine proximity to mineralization, and these may be useful in exploring for precious metal-rich VMS deposits elsewhere. Key criteria include (1) the presence of altered rhyodacitic rocks; (2) proximal to ore, alteration assemblages are typified by sericite-green mica-pyrite and sericite-quartz-pyrite, and peripheral to mineralization, alteration is quartz-calcite-garnet; (3) intense chlorite-stringer zone alteration occurs stratigraphically below and distal to some of the massive sulphide lenses — these lenses are commonly Cu-rich and Au-Ag-poor (e.g. Ming and East Mine deposits). It is also notable that there is a spatial "gap" between the chlorite-stringer zone alteration assemblage and the massive sulphide lenses. The Au-rich 1806 zone, and parts of the Ming South and 1807 zones, do not have associated advanced argillic alteration typical of other Au-rich VMS deposits (e.g. Bousquet 2-Dumagami; Dubé et al., 2014) They do, however, contain alteration assemblages similar to those in intermediate sulphidation VMS deposits (e.g. Eskay Creek: Roth et al., 1999). Characteristic ore minerals, such as tellurides and sulphosalts, can also be used as pathfinders for Au-enriched mineralization.

No major structural breaks have been identified southeast of the Ming deposit and there has been limited surface or subsurface exploration outside of the immediate deposit area; therefore, the prospectivity of the area outside of the immediate deposits remains high. It is now recognized that the Ming, Rambler Main, and East deposits are located at the top of the Rambler Rhyolite, at the contact with the overlying rocks of the Snooks Arm Group (Castonguay et al., 2009; Skulski et al., 2010). At or near (≤5 m from massive sulphide mineralization) this contact is an iron-rich sedimentary rock (Nugget Pond horizon) that serves as a regional "favourable" horizon and is a focus for exploration in the Rambler camp.

FUTURE WORK

Ongoing research on the Ming deposit focuses on the characterization of the petrogenesis and geochronology of the host rocks. Element mobility due to hydrothermal alteration will be characterized using lithogeochemical and optical reflectance spectroscopy on altered and unaltered host-rock samples. Structural relationships will be established using detailed underground mapping to determine the deformation history of the deposit and controls on the geometry and distribution of the ore.

ACKNOWLEDGEMENTS

This study was funded by the Targeted Geoscience Initiative (TGI-4) program of Natural Resources Canada. We sincerely thank Rambler Metals and Mining PLC (particularly L. Pilgrim and P. Legrow) for underground access and providing data. This research has also been financially supported by a Natural Sciences and Engineering Research Council of Canada (NSERC) Discovery Grant, by the NSERC-Altius Industrial Research Chair in Mineral Deposits supported by NSERC, Altius Resources Inc., and by the Research and Development Corporation of Newfoundland and Labrador. Thanks to P.-S. Ross and J.M. Peter for their careful reviews of this manuscript.

REFERENCES

Allen, R.L., Weihed, P., and Svenson, S.-A., 1996. Setting of Zn-Cu-Au-Ag massive sulfide deposits in the evolution and facies architecture of a 1.9 Ga marine volcanic arc, Skellefte District, Sweden; Economic Geology, v. 91, p. 1022–1053.

Brueckner, S.M., Piercey, S.J., Sylvester, P.J., Maloney, S., and Pilgrim, L., 2014a. Evidence for syngenetic precious metal enrichment in an Appalachian volcanogenic massive sulfide system: The 1806 zone, Ming mine, Newfoundland, Canada; Economic Geology, v. 109, p. 1611–1642.

Brueckner, S., Piercey, S., Layne, G., Piercey, G., and Sylvester, P., 2014b. Variations of sulphur isotope signatures in sulphides from the metamorphosed Ming Cu(-Au) volcanogenic massive sulphide deposit, Newfoundland Appalachians, Canada; Mineralium Deposita. doi: 10.1007/s00126-014-0567-7.

Castonguay, S., Skulski, T., van Staal, C., and Currie, M., 2009. New insights on the structural geology of the Pacquet Harbour group and Point Rousse complex, Baie Verte peninsula, Newfoundland, *In:* Current Research; Newfoundland and Labrador Department of Natural Resources, Geological Survey, Report 09-1, p. 147–158.

Cawood, P.A., van Gool, J.A.M., and Dunning, G.R., 1993. Silurian age for movement on the Baie Verte Line: Implications for accretionary tectonics in the Northern Appalachians, *In:* Abstract with Programs; Geological Society of America, v. 25, p. A422.

Dubé, B., Mercier-Langevin, P., Hannington, M.D., Lafrance, B., Gosselin, G., and Gosselin, P., 2007. The LaRonde Penna world-class Au-rich volcanogenic massive sulfide deposit, Abitibi, Quebec: mineralogy and geochemistry of alteration and implications for genesis and exploration; Economic Geology, v. 102, p. 633–666.

Dubé, B., Mercier-Langevin, P., Kjarsgaard, I., Hannington, M., Bécu, V., Côté, J., Moorhead, J., Legault, M., and Bédard, N., 2014. The Bousquet 2-Dumagami world-class Archean Au-rich volcanogenic massive sulfide deposit, Abitibi, Quebec: Metamorphosed submarine advanced argillic alteration footprint and genesis; Economic Geology, v. 109, p. 121–166.

Franklin, J.M., Gibson, H.L., Jonasson, I.R., and Galley, A.G., 2005. Volcanogenic massive sulfide deposits, *In:* Economic Geology 100th Anniversary Volume, (ed.) J.W. Hedenquist, J.F.H. Thompson, R.J. Goldfarb, and J.P. Richards; Society of Economic Geologists, Littleton, Colorado, p. 523–560.

Gemmell, J.B. and Fulton, R., 2001. Geology, genesis, and exploration implications of the footwall and hanging-wall alteration associated with the Hellyer volcanic-hosted massive sulfide deposit, Tasmania, Australia; Economic Geology, v. 96, p. 1003–1035.

Gibson, H.L., 2005. Volcano-Hosted Ore Deposits, *In:* Volcanoes and the Environment, (ed.) G.G.J. Ernst; Cambridge University Press, New York, New York, p. 333–386.

Gibson, H., Morton, R.L., and Hudak, G.J., 1999. Submarine volcanic processes, deposits, and environments favorable for the location of volcanic-associated massive sulfide deposits; Reviews in Economic Geology, v. 8, p. 13–51.

Hibbard, L.J., 1983. Geology of the Baie Verte Peninsula, Newfoundland; Department of Mines and Energy, Government of Newfoundland and Labrador, Memoir 2, 279 p.

Lydon, J.W., 1988. Volcanogenic massive sulphide deposits Part 2: Genetic models; Geoscience Canada, v. 15, p. 43–65.

Mercier-Langevin, P., Dubé, B., Hannington, M.D., Richer-Laflèche, M., and Gosselin, G., 2007. The LaRonde Penna Au-Rich volcanogenic massive sulfide deposit, Abitibi greenstone belt, Quebec: Part II. Lithogeochemistry and paleotectonic setting; Economic Geology, v. 102, p. 611–631.

Mercier-Langevin, P., Hannington, M.D., Dubé, B., and Bécu, V., 2011. The gold content of volcanogenic massive sulfide deposits; Mineralium Deposita, v. 46, p. 509–539.

Mercier-Langevin, P., Hannington, M.D., Dubé, B., Piercey, S.J., Peter, J.M., and Pehrsson, S.J., 2015. Precious metal enrichment processes in volcanogenic massive sulphide deposits — A summary of key features, with an emphasis on TIGI-4 research contributions, *In:* Targeted Geoscience Initiative 4: Contributions to the Understanding of Volcanogenic Massive Sulphide Deposit Genesis and Exploration Methods Development, (ed.) J.M. Peter and P. Mercier-Langevin; Geological Survey of Canada, Open File 7853, p. 117–130.

Ohmoto, H., 1996. Formation of volcanogenic massive sulfide deposits: The Kuroko perspective; Ore Geology Reviews, v. 10, p. 135–177.

Piercey, S.J., Jenner, G.A., and Wilton, D.H.C., 1997. The stratigraphy and geochemistry of the southern Pacquet Harbour Group, Baie Verte Peninsula, Newfoundland: Implications for mineral exploration, *In:* Current Research, (ed.) C.P.G. Pereira and D.G. Walsh; Newfoundland and Labrador Department of Mines and Energy, p. 119–139.

Pilgrim, L., 2009. Mineral Resource Estimate for the Ming Mine, Newfoundland, Canada; Rambler Metals and Mining Canada Ltd., unpublished technical report, p. 114.

Pilote, J.-L. and Piercey, S.J., 2013. Volcanostratigraphy of the 1807 zone of the Ming Cu-Au volcanogenic massive-sulphide deposit, Baie Verte Peninsula, northern Newfoundland; Geological Survey of Canada, Current Research 2013-20, 13 p. doi:10.4095/293128

Pilote, J.-L., Piercey, S.J., and Mercier-Langevin, P., 2014. Stratigraphy and hydrothermal alteration of the Ming Cu-Au volcanogenic massive-sulphide deposit, Baie Verte Peninsula, Newfoundland; Geological Survey of Canada, Current Research 2014-7, 18 p. doi:10.4095/295145

Poulsen, K.H. and Hannington, M.D., 1995. Volcanic-associated massive sulphide gold, *In:* Geology of Canadian Mineral Deposit Types, (ed.) O.R. Eckstrand, W.D. Sinclair, and R.I. Thorpe; Geological Survey of Canada, Geology of Canada Series no. 8, p. 183–196. doi:10.4095/207944

Poulsen, K.H., Robert, F., and Dubé, B., 2000. Geological Classification of Canadian Gold Deposits; Geological Survey of Canada, Bulletin 540, 113 p.

Ross, P.-S. and Mercier-Langevin, P., 2014. Igneous rock associations 14. The volcanic setting of VMS and SMS deposits: a review; Geoscience Canada, v. 41, p. 365–377.

Roth, T., Thompson, J.F.H., and Sillitoe, R.H., 1999. The precious metal-rich Eskay Creek deposit, northwestern British Columbia; Reviews in Economic Geology, v. 8, p. 357–373.

Skulski, T., Castonguay, S., McNicoll, V., van Staal, C., Kidd, W., Rogers, N., Morris, W., Ugalde, H., Slavinski, H., Spicer, W., Moussallam, Y., and Kerr, I., 2010. Tectonostratigraphy of the Baie Verte oceanic tract and its ophiolite cover sequence on the Baie Verte Peninsula, *In:* Current Research; Newfoundland and Labrador Department of Natural Resources, Geological Survey, Report 10-1, p. 315–335.

Tuach, J. and Kennedy, M.J., 1978. The geologic setting of the Ming and other sulfide deposits, consolidated Rambler mines, Northeast Newfoundland; Economic Geology, v. 73, p. 192–206.

van Staal, C.R. and Barr, S.M., 2012. Lithospheric architecture and tectonic evolution of the Canadian Appalachians and associated Atlantic margin, *In:* Tectonic Styles in Canada: The LITHOPROBE Perspective, (ed.) J.A. Percival, F.A. Cook, and R.M. Clowes; Geological Association of Canada, Special Paper 49, p. 41–96.

van Staal, C.R., Chew, D.M., Zagorevski, A., McNicoll, V., Hibbard, J., Skulski, T., Escayola, M.P., Castonguay, S., and Sylvester, P.J., 2013. Evidence of Late Ediacaran hyperextension of the Laurentian Iapetan margin in the Birchy Complex, Baie Verte Peninsula, Northwest Newfoundland: Implications for the opening of Iapetus, formation of Peri-Laurentian microcontinents and Taconic – Grampian orogenesis; Geoscience Canada, v. 40, p. 94–117.

White, J.D.L. and Houghton, B.F., 2006. Primary volcaniclastic rocks; Geology, v. 34, p. 677–680.

Williams, H., 1979. Appalachian orogen in Canada; Canadian Journal of Earth Sciences, v. 16, p. 792–807.